Research Square

Preprints are preliminary reports that have not undergone peer review.
They should not be considered conclusive, used to inform clinical practice,
or referenced by the media as validated information.

Linking Derivative Absorption Spectra and HPLC Pigments to Satellite Observations for Phytoplankton Typing in Coastal India

Aswathy Vijaya Krishna

achuvk@gmail.com

Space Applications Centre, ISRO https://orcid.org/0000-0002-1003-8446

Srijith B

VIKAS Centre for Development, Ahmedabad, India

Anima Tirkey

Department of Botany, Gujarat University, Ahmedabad, India

Syed Moosa Ali

Space Applications Centre, ISRO

Debojyoti Ganguly

Space Applications Centre, ISRO

Anurag Gupta

Space Applications Centre, ISRO

Mini Raman

Space Applications Centre, ISRO

Sanjib Kumar Deb

Space Applications Centre, ISRO

Rashmi Sharma

Space Applications Centre, ISRO

Research Article

Keywords: CHEMTAX, Coastal waters, Fourth derivative, HPLC, Phytoplankton absorption, Remote sensing

Posted Date: February 24th, 2026

DOI: https://doi.org/10.21203/rs.3.rs-8940255/v1

License: This work is licensed under a Creative Commons Attribution 4.0 International License.
Read Full License

Additional Declarations: The authors declare no competing interests.

Linking Derivative Absorption Spectra and HPLC Pigments to Satellite Observations for Phytoplankton Typing in Coastal India

Aswathy Vijaya Krishna[1*], Srijith B[2], Anima Tirkey[1,3], Syed Moosa Ali[1], Debojyoti Ganguly[1], Anurag Gupta[1], Mini Raman[1], Sanjib Kumar Deb[1], Rashmi Sharma[1]

[1]Space Applications Centre, Ahmedabad, India

[2]VIKAS Centre for Development, Ahmedabad, India

[3]Department of Botany, Gujarat University, Ahmedabad, India

**Corresponding author Email: aswathyvk@sac.isro.gov.in / achuvk@gmail.com*

Aswathy Vijaya Krishna- ORCID ID: 0000-0002-1003-8446

Statements and Declarations

Competing Interests: The authors declare that they have no conflict of interest.

Funding: Not applicable.

Data Availability Statement: *In-situ* data supporting this study are available in the article. Satellite data supporting this study are available in public domain sources: https://oceancolor.gsfc.nasa.gov/.

Author's contributions:

AVK-Conceptualization, Data curation, Formal analysis, Investigation, Methodology, Validation, Visualization, Writing-original draft, Writing- review & editing**; SB-** Data curation, Formal analysis, Methodology, Software, Validation, Visualization, Writing- review & editing**; AT-** Investigation, Validation, Visualization, Writing-review & editing**; SMA-** Data curation, Formal analysis**; DG-** Data curation, Formal analysis**; AG-** Data curation, Formal analysis**; MR-** Project administration, Supervision**; SKD-** Supervision, Writing- review & editing; **RS-** Supervision, Writing- review & editing.

Acknowledgement

23 The authors thank the Director, SAC (ISRO) and the former Deputy Director of EPSA, Dr. Raj Kumar, for their
24 support. We acknowledge the AVIRIS-NG team for their support, and Dr. Mohamed Hatha, CUSAT, for field
25 and lab assistance.

26

Linking Derivative Absorption Spectra and HPLC Pigments to Satellite Observations for Phytoplankton Typing in Coastal India

Abstract

The phytoplankton community structure in the coastal waters off Kochi during March 2018 was investigated using a comprehensive multi-technique approach that combined microscopy, high-performance liquid chromatography (HPLC) pigment analysis, CHEMTAX, phytoplankton absorption spectra, and fourth-derivative analysis. These complementary methods provided consistent insights into community composition, indicating diatom dominance in nearshore waters, with increasing contributions from cryptophytes and cyanobacteria offshore. Fourth-derivative analysis enhanced spectral resolution and enabled the identification of diagnostic pigment absorption features, including fucoxanthin associated with diatoms and zeaxanthin associated with cyanobacteria. Building on these *in-situ* observations, absorption-derived spectral features were extended to multispectral satellite reflectance to examine the spatial expression of dominant phytoplankton compositional contrasts across the coastal-offshore gradient. An absorption-guided two-stage framework was applied to isolate absorption-sensitive spectral structure from reflectance and relate it to relative pigment composition. The derived spectral proxies exhibited monotonic relationships with chlorophyll-normalized phytoplankton absorption and internally consistent associations with diagnostic pigment ratios, although predictive skill under cross-validation remained limited. The resulting pigment ratio fields revealed smooth coastal-offshore gradients that broadly aligned with relative *in-situ* pigment patterns and are therefore interpreted as illustrative of spatial coherence in relative phytoplankton compositional structure rather than as validated pigment estimates.

Keywords: CHEMTAX, Coastal waters, Fourth derivative, HPLC, Phytoplankton absorption, Remote sensing.

1. Introduction

Phytoplankton are key producers in marine ecosystems, and their composition significantly influences food web dynamics, biogeochemical cycles, and ocean colour. In optically complex coastal waters of India (Monolisha et al., 2018), understanding phytoplankton community structure is challenging due to high variability in water constituents and overlapping spectral features of pigments. Traditional microscopic methods, while informative, are often labour-intensive and limited in resolving smaller sized phytoplankton. Optical and biochemical

techniques such as phytoplankton absorption spectroscopy and high-performance liquid chromatography (HPLC) have emerged as powerful tools for characterizing phytoplankton diversity.

The absorption spectra of phytoplankton contain signatures of light-harvesting and accessory pigments, which vary across taxonomic groups (Hoepffner and Sathyendranath, 1991; Bricaud et al., 2004). Applying fourth derivative analysis to these spectra helps resolve overlapping peaks and enhances detection of subtle pigment features. Coupling HPLC pigment data with CHEMTAX analysis allows for the quantitative estimation of phytoplankton functional types (Mackey et al., 1996; Vidussi et al., 2001; Uitz et al., 2006; Hirata et al., 2011; Higgins et al., 2012). When combined with HPLC pigment measurements and CHEMTAX-based class composition estimates, absorption-derived spectral features provide a robust, internally consistent framework for characterizing phytoplankton communities at the point of observation (CHEMTAX; Mackey et al., 1996; Higgins et al., 2012).

Extending such *in-situ* characterizations to regional scales using satellite ocean-colour data remains challenging. Satellite ocean-colour sensors measure water-leaving radiance expressed as remote-sensing reflectance (R_{rs}), which integrates absorption and scattering by multiple optically active constituents within the water column (Morel and Prieur, 1977; Gordon et al., 1988). In optically complex coastal waters, pigment-related information is expressed indirectly through spectral shape rather than absolute magnitude, as phytoplankton absorption overlaps spectrally with coloured dissolved organic matter and non-algal particles (Bricaud et al., 1995; Babin et al., 2003; IOCCG, 2014).

Accordingly, this study investigates phytoplankton group composition in Indian coastal waters, focusing on the optically diverse coastal-offshore transition off Kochi, using an integrated approach combining phytoplankton absorption spectra, fourth-derivative analysis, HPLC-CHEMTAX classification, and satellite-derived optical information, with the aim of informing physically consistent phytoplankton functional type characterization from ocean-colour observations.

Conceptual scope and novelty

This study adopts a deliberately qualitative satellite framework to examine whether phytoplankton compositional contrasts inferred from *in-situ* optical and pigment observations manifest as coherent spatial structure in multispectral ocean-colour data. The satellite component is not intended to retrieve pigment concentrations or to evaluate predictive skill. Rather, it tests the persistence of an optical-compositional hierarchy under spatial aggregation and spectral compression inherent to multispectral sensors.

Previous studies have shown that, in optically complex coastal waters, multispectral reflectance is better suited to resolving dominant compositional contrasts than to independently estimating individual pigment concentrations (Hirata et al., 2011; IOCCG, 2014; Bracher et al., 2017). Consistent with this understanding, the present analysis focuses on absorption-guided reflectance shape descriptors and pigment-to-chlorophyll-a ratios as indicators of relative community composition. The satellite analysis therefore provides contextual spatial expression of *in-situ* observations, rather than independent ecological inference.

2. Materials and Methods

2.1. Study Area

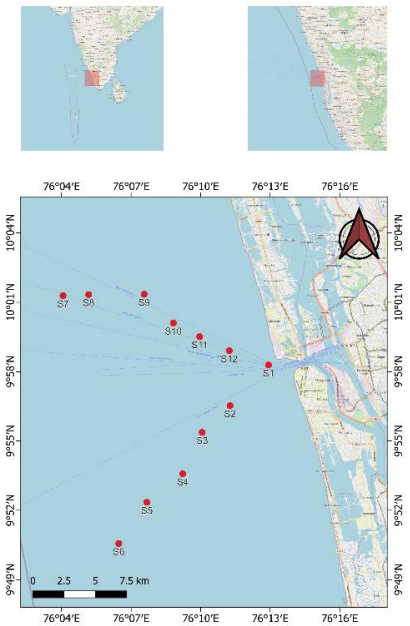


Fig. 1 Map showing the locations of sample collection.

In March 2018, sea-truth data were collected from 12 stations off Kochi (Fig. 1), Kerala, covering waters with varying optical properties. The Kochi bar mouth, connecting the backwaters and Arabian Sea, plays a key role in regulating water quality due to tidal mixing (Qasim and Gopinathan, 1969). The Periyar River, along with industrial discharges (Baby et al., 2024), influences the physicochemical and biological conditions of the Kochi backwaters, Vembanad Lake, and adjacent coastal waters.

2.2. Sampling and Analytical Procedures

- **Phytoplankton taxonomy:** Water samples (0.2 L) were preserved with Lugol's iodine and formaldehyde, concentrated to ~10-15 mL, and examined using a Zeiss® inverted microscope. Identification and enumeration were performed using standard taxonomic keys (Tomas, 1997).

- **Phytoplankton absorption:** GF/F filters were used to collect particulates from samples (0.1-1 L) under low vacuum in dim light and stored in liquid nitrogen. Optical density was measured spectrophotometrically with reference blank filters. Pathlength amplification was corrected (Stramski et al., 2015) and particulate absorption coefficients were derived. Filters were extracted thrice with warm methanol and filtered sea water to remove pigments. Post-extraction OD was measured to derive non-algal particulate absorption. Phytoplankton absorption was computed as the difference between total and de-pigmented absorption spectra (Neeley and Mannino, 2018).

- **Derivative Spectral Analysis:** Fourth derivative analysis of phytoplankton absorption spectra was performed using Savitzky-Golay smoothing with a 30-point, fourth-degree polynomial to reduce noise (Savitzky and Golay, 1964). Positive peaks in the derivative spectra, which correspond to pigment absorption maxima, were used for qualitative pigment identification.

- **Phytoplankton pigments (HPLC):** Water (0.1-1 L) was filtered (GF/F, 0.7 μm), stored in liquid nitrogen, and later at -80°C. Pigments were extracted in 90% acetone (Zapata et al., 2000), sonicated, centrifuged, and filtered (Vijaya Krishna et al., 2024). Analysis was performed using Agilent HPLC with a C8 column and diode array detector (440 and 660 nm). Pigments were identified via spectral and retention time match with 30 commercial standards (DHI Inc. Denmark).

- **CHEMTAX analysis:** Pigment data from surface samples were input into CHEMTAX (Mackey et al., 1996) using the initial pigment:chlorophyll-a ratio matrix provided by (Mackey et al, 1998). Optimal output was selected based on minimum RMS error and known phytoplankton composition in the study region.

- ***In-situ* Remote Sensing Reflectance (R_{rs}):** $R_{rs}(\lambda)$ measurements were obtained using a Satlantic (Inc.) underwater radiometer. The data were processed with Satlantic's HyperPro software, which calculates $R_{rs}(\lambda)$ as the ratio of upwelling radiance [$Lw(\lambda)$] to downwelling irradiance [$Ed(\lambda)$] just above the water surface.

$$Rrs = \frac{Lw(0+,\lambda)}{Ed(0+,\lambda)}$$

The radiometer data was used exclusively to characterize phytoplankton absorption features, perform fourth-derivative spectral analysis, and guide the selection of diagnostically relevant absorption anchor wavelengths.

2.3. Satellite Data Acquisition

Satellite remote sensing reflectance (R_{rs}) data of 4km resolution were obtained from 8-day (March 13–21, 2018) composite MODIS observations (https://oceancolor.gsfc.nasa.gov/). The use of 8-day composite MODIS R_{rs} data was necessitated by persistent cloud cover and coastal adjacency effects, which resulted in substantial data gaps and spatial masking in single-day imagery during the sampling period. Given that the objective of the satellite analysis was to resolve relative spatial gradients in phytoplankton compositional structure rather than instantaneous matchups or absolute retrievals, the use of temporally composited R_{rs} data is appropriate and consistent with previous coastal remote sensing studies (e.g., Pan et al., 2010; IOCCG, 2014).

2.4. Qualitative Compositional Inference Using an Absorption-Guided Two-Stage Optical Framework

Total absorption in natural waters can be expressed as the sum of contributions from pure water, coloured dissolved organic matter (CDOM), non-algal particles (NAP), and phytoplankton:

$$a(\lambda) = a_w(\lambda) + a_{CDOM}(\lambda) + a_{NAP}(\lambda) + a_{phy}(\lambda)$$

where a_w, a_{CDOM}, a_{NAP}, and a_{phy}represent absorption by pure water, coloured dissolved organic matter, non-algal particles, and phytoplankton, respectively. Among these components, only phytoplankton absorption directly encodes information on pigment composition and taxonomic structure.

Variations in phytoplankton pigment composition primarily influence the spectral shape of $a_{phy}(\lambda)$, whereas its absolute magnitude is largely controlled by phytoplankton biomass (Bricaud et al., 1995; Ciotti et al., 2002). To isolate compositional information from biomass effects, absorption analysis therefore emphasizes spectral shape descriptors rather than absolute absorption.

For this reason, log-ratio spectral shape descriptors (a^*_{phy}) guided by phytoplankton absorption structure were used. Normalization of these descriptors by chlorophyll-a further suppresses biomass variability, allowing absorption features associated with accessory pigments to be expressed more clearly (Bricaud et al., 2004).

This distinction is particularly important in optically complex coastal waters, where variability in chlorophyll concentration, suspended particles, and CDOM can mask pigment-specific absorption features when absolute absorption metrics are used (Babin et al., 2003; IOCCG, 2014). By focusing on normalized, absorption-guided spectral shape descriptors, the satellite framework remains sensitive to relative phytoplankton community composition rather than total phytoplankton abundance (Hirata et al., 2011).

The satellite framework described below therefore adheres explicitly to the qualitative scope and information limits defined in Section *Conceptual scope and novelty*.

Stage 1: Log-ratio spectral shape descriptor guided by phytoplankton absorption structure

Satellite remote-sensing reflectance (R_{rs}) represents the combined effects of absorption and scattering by multiple optically active constituents. Consequently, pigment-related information is expressed primarily through spectral structure rather than absolute reflectance magnitude.

To enhance sensitivity to absorption-driven spectral features while suppressing broadband illumination and scattering effects, log-transformed ratios of spectrally adjacent reflectance bands were used:

$$X(\lambda_i, \lambda_j) = \log_{10}\left(\frac{R_{rs}(\lambda_i)}{R_{rs}(\lambda_j)}\right)$$

where $X(\lambda_i, \lambda_j)$ represents the dimensionless value derived from reflectance at two wavelengths and $\frac{R_{rs}(\lambda_i)}{R_{rs}(\lambda_j)}$ is the ratio of reflectance measured at wavelengths $\lambda_i$and λ_j. Such log-ratio transformations reduce the influence of multiplicative effects and emphasize differential absorption features associated with pigment composition (Morel and Gentili, 1991; Gordon, 1997).

The resulting reflectance-based descriptors were related to chlorophyll-normalized phytoplankton absorption structure through a first-order linear statistical closure:

$$\hat{a}^*_{phy}(\lambda) = \beta_0 + \beta_1 X(\lambda_i, \lambda_j)$$

where $\hat{a}^*_{phy}(\lambda)$represents aspectral shape descriptor at wavelength λ, and $\beta_0, \beta_1$are fitted coefficients. This relationship is intended to preserve relative spectral structure.

Selection of diagnostically relevant wavelengths was guided by fourth-derivative analysis of *in-situ* phytoplankton absorption spectra, which consistently revealed curvature features in the blue (~440 nm), blue-green (~498 nm), and red (~681 nm) regions. Fourth-derivative analysis is used exclusively to guide wavelength selection and interpretation and is not propagated quantitatively into the satellite stage.

For satellite application, these absorption features were approximated using the nearest available multispectral bands. This approximation retains relative spectral structure while remaining consistent with the spectral limitations of multispectral sensors.

Stage 2: Log -ratio spectral shape descriptors to diagnostic pigment ratios

To examine phytoplankton compositional variability while minimizing biomass effects, diagnostic pigment composition was expressed using pigment-to-chlorophyll-a ratios. Pigment ratios are commonly used as indicators of relative phytoplankton functional composition, as they suppress first-order biomass dependence and emphasize changes associated with accessory pigment assemblages.

Pigment-to-chlorophyll-a ratios were related to the absorption-guided spectral shape descriptors derived in Stage 1 using log-linear statistical models of the form:

$$\log_{10}\left(\frac{P}{Chl\text{-}a}\right) = \alpha_0 + \sum_{k=1}^{3} \alpha_k \, \hat{a}^*_{phy}(\lambda_k)$$

where *P* represents a diagnostic pigment (e.g., zeaxanthin or fucoxanthin), $\hat{a}^*_{phy}(\lambda_k)$ are the absorption-guided spectral shape descriptors at the selected wavelengths λ_k, and $\alpha_0$and $\alpha_k$are fitted coefficients.

This formulation is intended to describe relative compositional structure rather than to retrieve absolute pigment

concentrations. By modeling pigment ratios instead of concentrations, the analysis remains focused on phytoplankton community composition and reduces sensitivity to variations in total phytoplankton biomass.

3. Results and Discussion

The analysis integrates *in-situ* and satellite-based observations to understand the spatial and spectral variability of phytoplankton communities in the coastal waters off Cochin. Taxonomic data, pigment composition, absorption characteristics, and remote sensing indices together reveal insights into the dominant phytoplankton groups and their optical signatures, influenced by local hydrography and anthropogenic inputs.

3.1. Phytoplankton composition and taxonomy

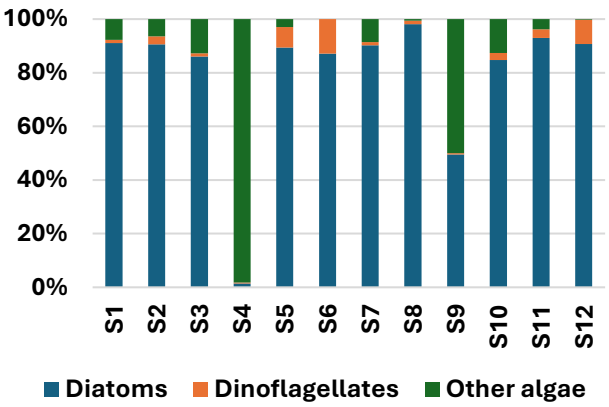


Fig. 2 Percentage contribution of diatoms, dinoflagellates and other algae across sampling locations.

Microscopic examination of surface water samples revealed a rich and diverse phytoplankton assemblage in the coastal waters off Cochin. Diatoms were the most dominant group, with frequent occurrences of *Skeletonema, Rhizosolenia, Guinardia, Pseudo-nitzschia, Chaetoceros, Eucampia, Thalassiosira, Thalassionema, Nitzschia* and *Dactyliosolen* species across most stations. Dinoflagellates such as *Alexandrium, Ceratium, Prorocentrum, Heterocapsa, Protoperidinium* and *Gonyaulax* were also present, particularly in stations near the estuarine influence. Smaller groups, including dictyocophytes, chrysophytes, and cyanobacteria (*Crocosphaera watsonii* and unidentified beaded chained cells), were observed in moderate abundance, especially in the offshore waters. Bloom of cyanobacteria, *Trichodesmium thiebautii* was observed at S4 with very high cell density (7.04 x 10^6 trichome l^{-1}) which contributed 98% of the total phytoplankton population. Unidentified long beaded chained cells

of cyanobacteria was observed at S9 which contributed almost 50% of total phytoplankton population. The taxonomic composition varied distinctly with station characteristics (Fig. 2), with nearshore sites dominated by diatoms and dinoflagellates, while offshore stations exhibited a community structure typical of open ocean environments (Reddy et al., 2024).

3.2. Pigment composition and CHEMTAX-derived groups

HPLC analysis (Fig. 3) confirmed the dominance of chlorophyll-a (chl-a), which varied significantly across stations, with higher values observed in inshore and bar-mouth regions. Fucoxanthin (fuco) was the most abundant accessory pigment, indicating the prevalence of diatoms. Chlorophyll-b, peridinin, alloxanthin and zeaxanthin (zea) were also notable, suggesting contributions from chlorophytes, dinoflagellates, cryptophytes and cyanobacteria, respectively. The presence of divinyl chlorophyll-a at few offshore stations indicated the presence of prochlorophytes. These results are consistent with those reported by (Vijayan et al., 2021) for the eastern Arabian Sea. Regions characterized by low salinity and elevated nutrient levels tend to support the dominance of larger phytoplankton such as diatoms, while areas with higher salinity and limited nutrient availability are typically inhabited by smaller phytoplankton like cyanobacteria (Li et al., 2013; Zhang et al., 2013).

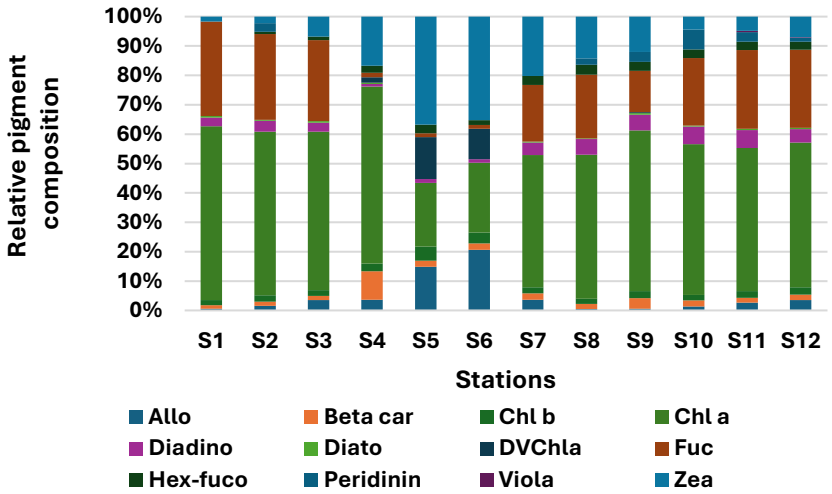


Fig. 3 Relative phytoplankton pigment distribution across sampling locations.

CHEMTAX analysis was performed using the pigment ratio matrix from (Mackey et al., 1998), specifically for surface waters (Fig. 4). The analysis estimated that diatoms contributed the highest proportion to chl-a biomass except at S5 and S6, followed by cryptophytes and cyanobacteria. Dinoflagellates, haptophytes and chrysophytes

contributed marginally. The spatial distribution showed a higher relative contribution of diatoms near the bar-mouth, likely driven by availability of nutrients due to estuarine influence. In contrast, smaller sized phytoplankton like cryptophytes and cyanobacteria dominated the offshore stations possibly due to the stratified nature of the water column. Previous studies in the coastal waters of the eastern Arabian Sea have identified diatoms and cyanobacteria as the major contributors, based on CHEMTAX analysis (Vijayan et al., 2021), whereas (Ahmed et al., 2016) reported a significant contribution of cryptophytes, particularly in the south-eastern region.

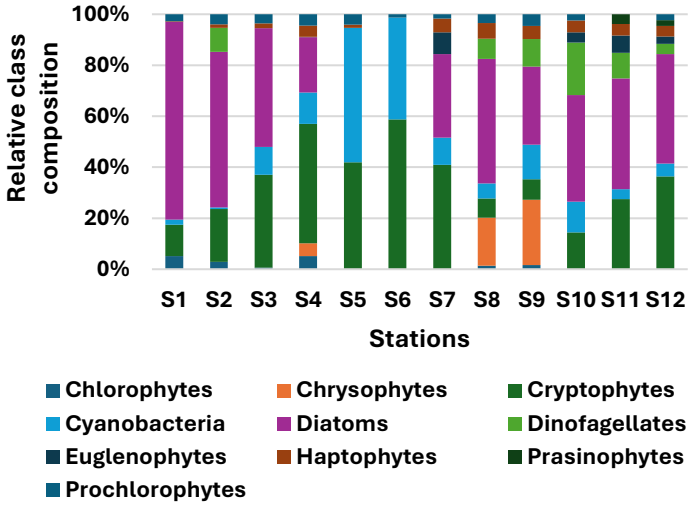


Fig. 4 Relative phytoplankton class composition across sampling locations.

3.3. Phytoplankton absorption and spectral features

Spectrophotometric measurements of total and de-pigmented particulate absorption revealed typical phytoplankton absorption spectra with prominent peaks at ~440 nm and ~675 nm, corresponding to chl-a. At 440 nm, the chl-a specific absorption coefficient (a*ph) exhibited notable variability across stations, ranging from 0.05 to 0.39 $m^2 mg^{-1}$, with the peak value detected at Station S5. Distinct secondary absorption peaks observed in the blue and green regions are attributed to accessory pigments such as fuco, peridinin and zea. The observed variations in absorption features reflect shifts in phytoplankton community composition and cell size distribution (Bidigare et al., 1990; Bricaud et al., 1995; Wang et al., 2015). As evident from Fig. 5, the phytoplankton community at S5 and S6 was predominantly composed of smaller-sized cells.

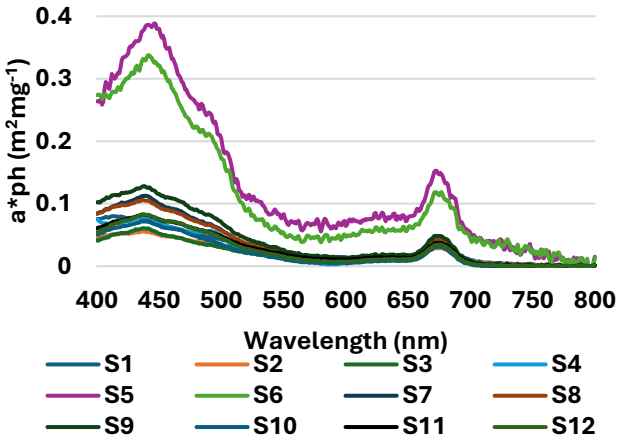


Fig. 5 Phytoplankton specific absorption coefficient across sampling sites.

The fourth-derivative analysis significantly enhanced the spectral resolution of the phytoplankton absorption spectra, allowing the identification of additional absorption peaks linked to specific diagnostic pigments. Figure 6 illustrates the fourth-derivative spectra from selected stations. At the coastal station S1 (Fig. 6a), numerous well-defined peaks were observed, indicative of high pigment diversity and, by extension, a complex phytoplankton community structure. Notable peaks include those associated with fuco (~520-530 nm), zexa (~480–490 nm), and chlorophyll-b (~648 nm), suggesting the dominance of diatoms, cyanobacteria and chlorophytes (Lorenzoni et al., 2015; Perez et al., 2007).

In contrast, the derivative spectra at station S4 (Fig. 6b), where a bloom of *Trichodesmium thiebautii* was identified, revealed characteristic absorption features at ~490, ~550, ~560, and ~615 nm. These correspond to zea, phycoerythrobilin, phycoerythrin, and phycocyanin, respectively (McKinna et al., 2015; Lorenzoni et al., 2015; Perez et al., 2007), reflecting the presence of cyanobacteria with rich phycobiliprotein content. Meanwhile, the offshore station (Fig. 6c) exhibited fewer absorption features, indicating lower pigment diversity. The absorption features identified through derivative analysis were consistent with HPLC-derived pigment compositions, thereby validating the presence and distribution of distinct phytoplankton groups across different stations.

The fourth-derivative technique proved effective in separating overlapping absorption bands, especially in optically complex coastal waters where coloured dissolved organic matter (CDOM) and non-algal particles often obscure pigment signals. The enhanced spectral resolution offers potential for identifying specific phytoplankton groups, especially when supported by pigment data.

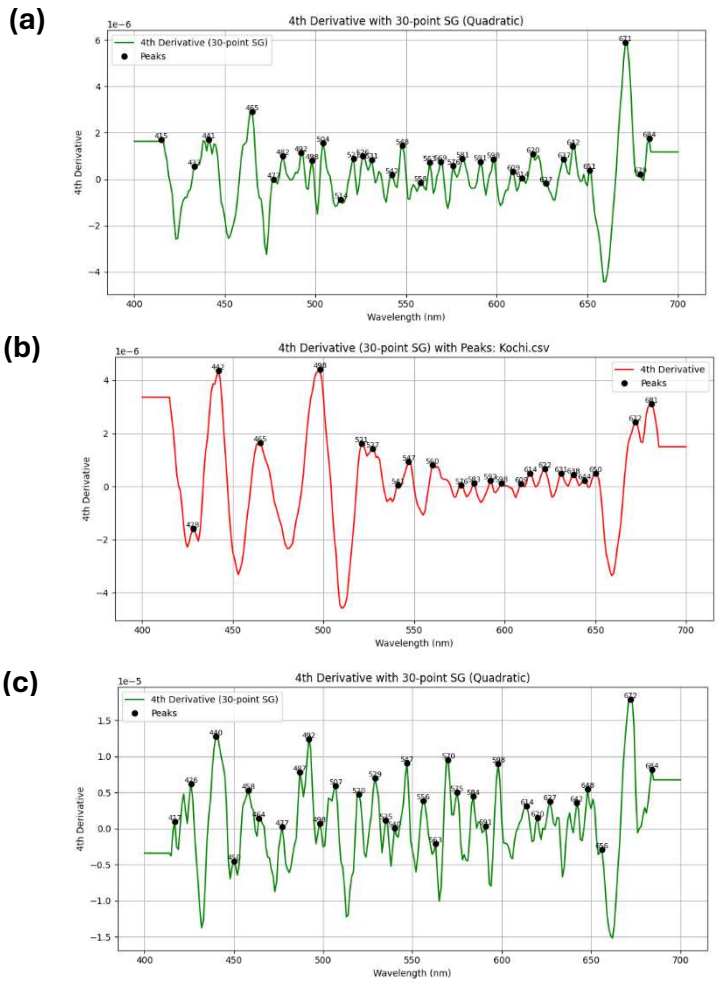


Fig. 6 Absorption peaks determined using 4th derivative analysis at (a) S1, (b) S4 and (b) S7.

3.4. Absorption-Guided Compositional Inference from Multispectral Reflectance

Multispectral satellite reflectance was analysed using the absorption-guided framework to examine whether compositional information inferred from *in-situ* observations is expressed as coherent spectral and spatial structure. Results are presented separately for the behaviour of log-ratio spectral shape descriptor guided by phytoplankton absorption structure, their statistical relationship with pigment ratios, and the resulting spatial patterns.

3.4.1. Behaviour of Stage-1 absorption-sensitive spectral proxies

The behaviour of Stage-1 absorption-sensitive spectral proxies is illustrated in Fig. 7, which compares proxy

values derived from multispectral reflectance with measured chlorophyll-normalized phytoplankton absorption at the corresponding wavelengths.

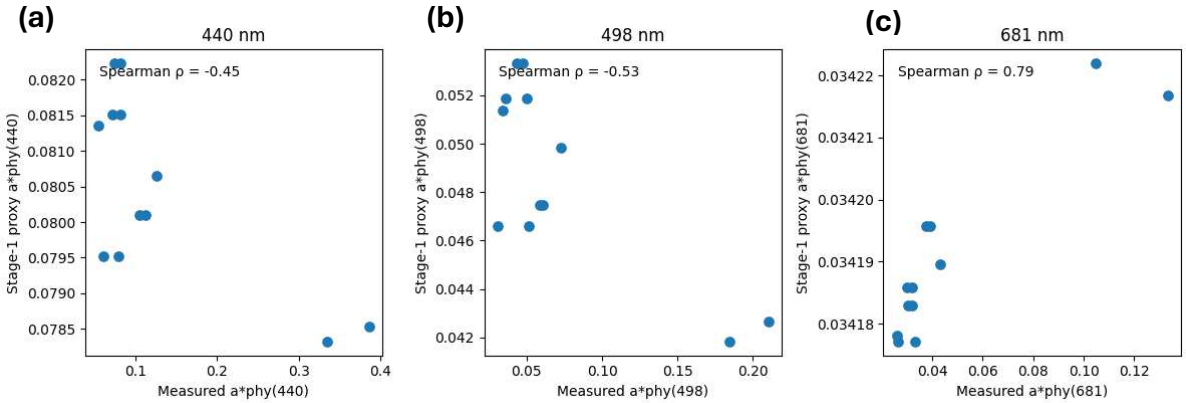


Fig. 7 Comparison between measured specific phytoplankton absorption and Stage-1 log-ratio spectral shape descriptor guided by phytoplankton absorption structure at (a) 440, (b) 498, and (c) 681 nm.

At 440 nm and 498 nm, the proxies exhibit moderate inverse monotonic relationships with measured a*phy, with Spearman rank correlation coefficients of −0.45 and −0.53, respectively (Fig. 7a–b). In contrast, the red-region proxy at 681 nm shows a positive monotonic relationship with measured a*phy, with a Spearman correlation coefficient of 0.79 (Fig. 7c).

Across all wavelengths, the proxy values span a substantially narrower dynamic range than the corresponding *in-situ* absorption measurements, indicating compression of amplitude information. The observed relationships are monotonic rather than linear, confirming that the proxies encode relative spectral structure rather than absolute absorption magnitude.

3.4.2. Stage-2 pigment ratio inference and validation

Log-ratio spectral shape descriptor guided by phytoplankton absorption structure were related to diagnostic pigment-to-chlorophyll-a ratios using log-linear statistical models. For both Zeaxanthin/Chl-a and Fucoxanthin/Chl-a, regression coefficients exhibited stable signs and relative magnitudes across cross-validation folds, indicating internally consistent compositional structure.

However, leave-one-out cross-validation yielded negative coefficients of determination (LOO $R^2 \approx -0.18$) and RMSE values of 0.57 for Zeaxanthin/Chl-a and 0.50 for Fucoxanthin/Chl-a, based on 12 samples. Given the negative cross-validated R^2 values, these relationships are interpreted strictly in terms of relative compositional contrast and internal consistency, consistent with the qualitative scope defined earlier.

Table. 1 Cross-validation statistics for Stage-2 pigment ratio models (LOO R^2, RMSE, sample size).

Target pigment ratio	Regression form	LOO R^2	LOO RMSE	Sample size (n)
Zea/Chla	log10(Zea/Chl-a) = -0.6973 − 0.0617·a*phy(440) − 0.0373·a*phy(498) − 0.0287·a*phy(681)	-0.18	0.57	12
Fuco/Chla	log10(Fuco/Chl-a) = -0.5961 + 0.0365·a*phy(440) + 0.0209·a*phy(498) + 0.0160·a*phy(681)	-0.18	0.50	12

3.4.3. Spatial distribution of pigment ratios

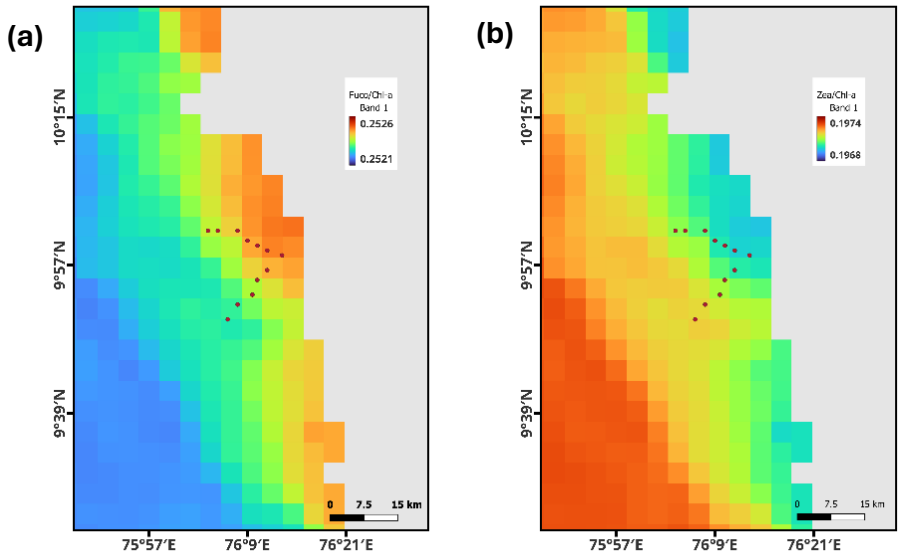


Fig. 8 Spatial distribution of (a) Fucoxanthin/Chl-a and (b) Zeaxanthin/Chl-a (dimensionless ratios). Maps illustrate relative spatial coherence only and do not represent validated pigment ratios

The spatial patterns of diagnostic pigment ratios derived from multispectral reflectance are shown in Fig. 8, which presents the mapped distributions of Fuco/Chl-a and Zea/Chl-a across the study region. The two fields together

delineate a dominant spatial contrast across the coastal-offshore transect, with the sampling locations overlaid on the maps falling within the corresponding gradient zones. The mapped fields are spatially smooth, reflecting the use of temporally composited satellite reflectance, and are interpreted in terms of persistent spatial patterns rather than point-scale variability.

The Fuco/Chl-a field (Fig. 8a) exhibits relatively higher values in nearshore waters that decrease offshore, forming a coherent coastal-offshore gradient. In contrast, the Zea/Chl-a field (Fig. 8b) displays an opposing spatial pattern, with comparatively higher values offshore and lower values in nearshore regions. These spatial distributions are consistent with the relative pigment composition observed at the sampling stations (Fig. 3), where stations S5 and S6 show enhanced zeaxanthin dominance, as reflected in Fig. 8b, while stations S1, S2, S11, and S12 exhibit relatively higher fucoxanthin dominance, consistent with Fig. 8a. Accordingly, these fields are interpreted as illustrative of spatial coherence in relative pigment gradients rather than as independent indicators of ecological inference.

4. Conclusion

The integration of microscopic taxonomy, pigment composition, CHEMTAX-derived functional group estimates, and phytoplankton absorption spectra offered a comprehensive understanding of the phytoplankton community structure in the optically complex waters off Kochi. The diatoms represented by fucoxanthin dominated the nearshore waters, while cryptophytes and cyanobacteria were more prevalent offshore. The consistency among these independent approaches reinforces the reliability of optical methods for distinguishing phytoplankton groups. Furthermore, the absorption-guided, normalized reflectance framework provides a qualitative means of examining spatial patterns in phytoplankton community composition using multispectral satellite data. The framework depict relative compositional gradients that are consistent with *in-situ* optical and pigment observations. Extension to hyperspectral satellite observations and expanded *in-situ* datasets may improve spectral discrimination and robustness while retaining the staged structure of the approach. Treating pigment-to-chlorophyll-a ratios as indicators of functional phytoplankton composition provides a qualitative framework for examining persistent compositional contrasts in optically complex coastal waters, rather than for detecting or predicting bloom events.

References

1. Ahmed, A., Kurian, S., Gauns, M., Chandrasekhararao, A.V., Mulla, A., Naik, B., Naik, H., & Naqvi, S.W.A. (2016). Spatial variability in phytoplankton community structure along the eastern Arabian Sea during the onset of south-west monsoon. *Continental Shelf Research*, 119, 30–39. https://doi.org/10.1016/j.csr.2016.03.005

2. Babin, M., Stramski, D., Ferrari, G.M., Claustre, H., Bricaud, A., Obolensky, G., & Hoepffner, N. (2003). Variations in the light absorption coefficients of phytoplankton, nonalgal particles, and dissolved organic matter in coastal waters around Europe. Journal of Geophysical Research: Oceans, 108(C7), 3211. https://doi.org/10.1029/2001JC000882

3. Bidigare, R.R., Ondrusek, M.E., Morrow, J.H. & Kiefer, D.A. (1990). In vivo absorption properties of algal pigments. *Deep-Sea Research Part A*, 37, 290–302.

4. Bracher, A., Bouman, H.A., Brewin, R.J.W., Bricaud, A., Brotas, V., Ciotti, A.M., & Woolley, A.R. (2017). Obtaining phytoplankton diversity from ocean colour: A scientific roadmap for future development. Frontiers in Marine Science, 4, 55. https://doi.org/10.3389/fmars.2017.00055

5. Bracher, A., Bouman, H.A., Brewin, R.J.W., Bricaud, A., Brotas, V., Ciotti, A.M., Clementson, L., Devred, E., Di Cicco, A., Dutkiewicz, S., Hardman-Mountford, N.J., Hickman, A.E., Hieronymi, M., Hirata, T., Losa, S.N., Mouw, C.B., Organelli, E., Raitsos, D.E., Uitz, J., Vogt, M., & Wolanin, A. (2017). Obtaining phytoplankton diversity from ocean color: A scientific roadmap for future development. Frontiers in Marine Science, 4, 55. https://doi.org/10.3389/fmars.2017.00055

6. Bricaud, A., Babin, M., Morel, A. & Claustre, H. (1995). Variability in the chlorophyll-specific absorption coefficients of natural phytoplankton: Analysis and parameterization. *Journal of Geophysical Research*, 100, 13321–13332.

7. Bricaud, A., Claustre, H., Ras, J. & Oubelkheir, K. (2004). Natural variability of phytoplanktonic absorption in oceanic waters: Influence of the size structure of algal populations. *Journal of Geophysical Research*, 109, C11010. https://doi.org/10.1029/2004JC002419

8. Gordon, H.R. (1997). Atmospheric correction of ocean color imagery in the Earth Observing System era. Journal of Geophysical Research: Atmospheres, 102(D14), 17081–17106. https://doi.org/10.1029/96JD02443

9. Gordon, H.R., Brown, J.W., & Evans, R.H. (1988). Exact Rayleigh scattering calculations for use with the Nimbus-7 Coastal Zone Color Scanner. Applied Optics, 27, 862–871.

10. Higgins, H.W., Wright, S.W. & Schlüter, L. (2012). Quantitative interpretation of chemotaxonomic pigment data. In: Roy, S., Llewellyn, C., Egeland, E.S. & Johnsen, G. (eds.), *Phytoplankton Pigments*. Cambridge University Press, Cambridge, pp. 257–313.

11. Hirata, T., Hardman-Mountford, N. J., Brewin, R. J. W., Aiken, J., Barlow, R., Suzuki, K., Isada, T., Howell, E., Hashioka, T., Noguchi-Aita, M., and Yamanaka, Y. (2011) Synoptic relationships between surface Chlorophyll-*a* and diagnostic pigments specific to phytoplankton functional types, *Biogeosciences*, 8, 311–327, https://doi.org/10.5194/bg-8-311-2011.

12. Hoepffner, N. & Sathyendranath, S. (1991). Effect of pigment composition on absorption properties of phytoplankton. *Marine Ecology Progress Series*, 73, 11–23. https://doi.org/10.3354/meps073011

13. IOCCG (2014). *Phytoplankton functional types from space*. Reports of the International Ocean-Colour Coordinating Group No. 15, Sathyendranath, S. (ed.), IOCCG, Dartmouth, Canada.

14. Li, L., Lu, S.H., Jiang, T. & Li, X. (2013). Seasonal variation of size-fractionated phytoplankton in the Pearl River estuary. *Chinese Science Bulletin*, 58, 2303–2314.

15. Libin Baby, Liya Jose, M.A. Solomon & P.T. Lakshmanan (2024). A study on total mercury content in surface water and backwater fishes of Periyar. *International Journal of Innovative Science and Research Technology*, 9(8), 1865. https://doi.org/10.38124/ijisrt/IJISRT24AUG1252

16. Lorenzoni, L., Toro-Farmer, G., Varela, R., Guzman, L., Rojas, J., Montes, E. & Muller-Karger, F. (2015). Characterization of phytoplankton variability in the Cariaco Basin using spectral absorption, taxonomic and pigment data. *Remote Sensing of Environment*, 167, 259–268.

17. Lotliker AA, Baliarsingh SK, Trainer VL, Wells ML, Wilson C, Udaya Bhaskar TVS, Samanta A, Shahimol SR. Characterization of oceanic Noctiluca blooms not associated with hypoxia in the Northeastern Arabian Sea. Harmful Algae. 2018 Apr;74:46-57. doi: 10.1016/j.hal.2018.03.008. Epub 2018 Apr 11. PMID: 29724342.

18. Mackey, D.J., Higgins, H.W., Mackey, M.D. & Holdsworth, D. (1998). Algal class abundances in the western equatorial Pacific: Estimation from HPLC measurements of chloroplast pigments using CHEMTAX. *Deep-Sea Research Part I*, 45, 1441–1468.

19. Mackey, M.D., Mackey, D.J., Higgins, H.W. & Wright, S.W. (1996). CHEMTAX—A program for estimating class abundances from chemical markers: Application to HPLC measurements of phytoplankton. *Marine Ecology Progress Series*, 144, 265–283. https://doi.org/10.3354/meps144265

20. Matondkar, S.G.P., Basu, S., Parab, S.G., Pednekar, S., Dwivedi, R.M., Raman, M., Goes, J.I., & Gomes, H. (2012). The bloom of the dinoflagellate *Noctiluca miliaris* in the North Eastern Arabian Sea: Ship and satellite study. *Proceedings of the 11th Pan Ocean Remote Sensing Conference*, 1–45.

21. McKinna, L.I.W. (2015). Three decades of ocean-colour remote sensing of *Trichodesmium* spp. in the world's oceans: A review. *Progress in Oceanography*, 131, 177–199.

22. Monolisha, M.S., Platt, T., Sathyendranath, S., Jayasankar, J., George, G. & Jackson, T. (2018). Optical classification of the coastal waters of the northern Indian Ocean. *Frontiers in Marine Science*, 5, 87. https://doi.org/10.3389/fmars.2018.00087

23. Morel, A., & Gentili, B. (1991). Diffuse reflectance of oceanic waters: Its dependence on Sun angle as influenced by the molecular scattering contribution. Applied Optics, 30(30), 4427–4438. https://doi.org/10.1364/AO.30.004427

24. Morel, A., & Prieur, L. (1977). Analysis of variations in ocean color. Limnology and Oceanography, 22(4), 709–722. https://doi.org/10.4319/lo.1977.22.4.0709

25. Neeley, R. & Mannino, A. (eds.) (2018). Inherent optical property measurements and protocols: Absorption coefficient. *IOCCG Ocean Optics and Biogeochemistry Protocols for Satellite Ocean Colour Sensor Validation*, IOCCG, Dartmouth.

26. Pan, X., Mannino, A., Russ, M.E., Hooker, S.B. & Harding, L.W. (2010). Remote sensing of phytoplankton pigment distribution in the United States northeast coast. *Remote Sensing of Environment*, 114, 2403–2416.

27. Perez, G., Queimaliños, C., Balseiro, E. & Modenutti, B. (2007). Phytoplankton absorption spectra along the water column in deep North Patagonian Andean lakes (Argentina). *Limnologica*, 37, 3–16.

28. Qasim, S.Z. & Gopinathan, C.K. (1969). Tidal cycle and environmental features of Cochin Backwater (a tropical estuary). *Proceedings of the Indian Academy of Sciences*, 69, 336–348.

29. Reddy, B.B., Vijayan, A.K., Sudheesh, V., Sherin, C.K., Roy, R., Vishnu, N.N., & Gupta, G.V.M. (2024). Nutrient stoichiometry drives the phytoplankton populations during the progression of upwelling along the eastern Arabian Sea. *Progress in Oceanography*, 229, 103347. https://doi.org/10.1016/j.pocean.2024.103347

30. Savitzky, A. & Golay, M.J.E. (1964). Smoothing and differentiation of data by simplified least squares procedures. *Analytical Chemistry*, 36, 1627–1639. https://doi.org/10.1021/ac60214a047

31. Stramski, D., Reynolds, R.A., Kaczmarek, S., Uitz, J. & Zheng, G. (2015). Correction of pathlength amplification in the filter-pad technique for measurements of particulate absorption coefficient in the visible spectral region. *Applied Optics*, 54, 6763–6782.

32. Tirkey, A., Vijaya Krishna, A., Srijith, B., Babu, K.N., Sahay, A., Solanki, H. & Alakes, A.S. (2025). Spectral deconvolution of green *Noctiluca* bloom pigments via fourth-derivative analysis: A step toward dedicated remote sensing algorithms. *Proceedings of INGARSS 2025*.

33. Tomas, C.R. (1997). *Identifying marine phytoplankton*. Academic Press, Toronto.

34. Uitz, J., Claustre, H., Morel, A. & Hooker, S.B. (2006). Vertical distribution of phytoplankton communities in the open ocean: An assessment based on surface chlorophyll. *Journal of Geophysical Research*, 111, C08005. https://doi.org/10.1029/2005JC003207

35. Vidussi, F., Claustre, H., Manca, B.B., Luchetta, A. & Marty, J. (2001). Phytoplankton pigment distribution in relation to upper thermocline circulation in the eastern Mediterranean Sea during winter. *Journal of Geophysical Research: Oceans*, 106, 19939–19956. https://doi.org/10.1029/1999JC000308

36. Vijaya Krishna A, Tirkey A, Raman M, Moosa Ali S, Sahay A, Singh A. (2024) Unravelling pre-monsoon phytoplankton: pigment profiles and community structure in the western and central Bay of Bengal. *Marine & Freshwater Research* 75, MF24103. https://doi.org/10.1071/MF24103

37. Vijayan, A.K., Reddy, B.B., Sudheesh, V., Marathe, P.H., Nampoothiri, V.N., Harikrishnachari, N.V., Kavya, P., Gupta, G.V.M., & Ramanamurthy, M.V. (2021). Phytoplankton community structure in a contrasting physico-chemical regime along the eastern Arabian Sea during the winter monsoon. *Journal of Marine Systems*, 215, 103501. https://doi.org/10.1016/j.jmarsys.2020.103501

38. Vijayan, K. & Somayajula, S.A. (2014). Effect of accessory pigment composition on the absorption characteristics of a dinoflagellate bloom in a coastal embayment. *Oceanologia*, 56, 107–124.

39. Wang, S., Ishizaka, J., Hirawake, T., Watanabe, Y., Zhu, Y., Hayashi, M., & Yoo, S. (2015). Remote estimation of phytoplankton size fractions using the spectral shape of light absorption. *Optics Express*, 23(8), 10301–10318. https://doi.org/10.1364/OE.23.010301

40. Zapata, M., Rodríguez, F. & Garrido, J.L. (2000). Separation of chlorophylls and carotenoids from marine phytoplankton: A new HPLC method using a reversed-phase C8 column and pyridine-containing mobile phases. *Marine Ecology Progress Series*, 195, 29–45.

41. Zhang, X., Huang, X.P., Shi, Z., Ye, F. & Liu, Q.X. (2013). Spatial and temporal variation of picophytoplankton in the Pearl River Estuary. *Acta Ecologica Sinica*, 33, 2200–2211.